Understanding meso-scale processes at a mixed-energy tidal inlet: Ameland Inlet, the Netherlands – Implications for coastal maintenance

Elias, Edwin P.L.; Pearson, S.G.; van der Spek, A.J.F.; Pluis, Stefan

DOI
10.1016/j.ocecoaman.2022.106125

Publication date
2022

Document Version
Final published version

Published in
Ocean & Coastal Management

Citation (APA)
Elias, E. P. L., Pearson, S. G., van der Spek, A. J. F., & Pluis, S. (2022). Understanding meso-scale processes at a mixed-energy tidal inlet: Ameland Inlet, the Netherlands – Implications for coastal maintenance. *Ocean & Coastal Management*, *222*, Article 106125. https://doi.org/10.1016/j.ocecoaman.2022.106125

Ocean and Coastal Management 222 (2022) 106125

Contents lists available at ScienceDirect

Ocean and Coastal Management

journal homepage: www.elsevier.com/locate/ocecoaman

Understanding meso-scale processes at a mixed-energy tidal inlet: Ameland Inlet, the Netherlands – Implications for coastal maintenance

Edwin P.L. Elias [a,*], Stuart G. Pearson [a,b], Ad J.F. van der Spek [a,c], Stefan Pluis [d]

[a] Deltares, P.O. Box 177, 2600 MH, Delft, the Netherlands
[b] Faculty of Civil Engineering and Geosciences, Delft University of Technology, PO Box 5048, 2600 GA, Delft, the Netherlands
[c] Faculty of Geosciences, Utrecht University, PO Box 80115, 3508 TC, Utrecht, the Netherlands
[d] Rijkswaterstaat, 3500 GE, Utrecht, the Netherlands

ARTICLE INFO

Keywords:
Wadden sea
Tidal inlets
Ebb-tidal delta

ABSTRACT

For successful and sustainable management of barrier islands, a thorough understanding of the ebb-tidal delta dynamics and interactions with the adjacent shorelines are of the utmost importance. Such understanding requires detailed observations and interpretations of the morphodynamics of smaller-scale features such as the individual channels and shoals (referred to as intra-delta dynamics). The intra-delta dynamics of Ameland Inlet (the Netherlands) are studied through analysis of sixteen high-resolution bathymetric surveys, supplemented with an extensive dataset of hydrodynamic observations collected in 2017. The observations are compiled into a synthesis of the morphodynamics of the ebb-tidal delta and its neighboring shorelines, to provide a basis for present day and future coastal management.

Our observations show that Ameland Inlet as a whole can be classified as a typical mixed-energy, wave-dominated system. However, the ebb-tidal delta contains distinct areas that are wave or tide dominated, and these areas evolve with the changing morphodynamics of the ebb delta. Between 2005 and 2021, large morphodynamic changes have occurred on the ebb-tidal delta and continuous erosion of the island tips occurred. Limited wave-sheltering by the ebb-tidal delta exposes the shorelines of the adjacent barrier islands to significant wave-driven sand transports and sand losses. Sediment supply from longshore transport and the erosion of the updrift island Terschelling contributed to the formation, growth and migration of a series of ebb-chutes and lobes, which eventually led to complete relocation of the main channel on the ebb-tidal delta. This main channel relocation took 15 years to complete and is an example of the ebb-delta breaching model of sand bypassing. Changes in the sediment bypassing patterns result in a sediment starved western island tip of Ameland, necessitating repeated sand nourishments under the Dutch coastal maintenance policy. Our observations also confirm the role the ebb-tidal delta as a sand reservoir for the downdrift barrier island. The delta sand body is not a reservoir for the back-barrier basin, since the basin is predominantly supplied with sand eroded from the updrift island of Terschelling.

As demonstrated in this study, the intra-delta dynamics of an ebb-tidal delta are complex and can change drastically through time. Only through detailed measurements and observations can all the intricate interactions that take place be unravelled.

1. Introduction and objective

Ebb-tidal deltas are large accumulations of sand that occur seaward of tidal inlets. The gross ebb-tidal delta volume might be related to tides or tidal prism (e.g., Hayes, 1975; Oertel, 1975; Walton and Adams, 1976), but waves are an important factor as they redistribute the sediments and contribute to the sediment bypassing mechanism (FitzGerald, 1988). Sediment transports are directly influenced by breaking of obliquely incident waves that generate currents, and due to wave asymmetry. Indirectly, waves enhance bed-shear stresses and stir up sediment, allowing more sediment to be suspended and subsequently transported by the tidal and wind-driven flows. The shape of the ebb-tidal delta reflects the ratio of the wave and tidal energy (e.g. Hayes 1975, 1979; Davis and Hayes, 1984; Oertel, 1975).

* Corresponding author.
E-mail address: edwin.elias@deltares.nl (E.P.L. Elias).

https://doi.org/10.1016/j.ocecoaman.2022.106125
Received 1 April 2021; Received in revised form 3 February 2022; Accepted 14 February 2022
Available online 18 March 2022

Ebb-tidal deltas are not only passive reservoirs of sand, but they also participate dynamically in exchanges of sand in and around tidal inlets. Shoreline variability of the adjacent barrier islands is for a major part directly related to the channel and shoal dynamics of the ebb-tidal delta (e.g. FitzGerald et al., 1984; Dean, 1988; FitzGerald, 1996; Hayes and FitzGerald, 2013; Elias et al., 2019).

Despite the complexity and dynamics of the ebb-tidal delta system, classification is often simple and based on geomorphic and/or hydrodynamic parameters (Bruun and Gerritsen, 1960; Hayes, 1979; Hubbard et al., 1979). A commonly used classification is that of Hayes (1979) in which mean tidal range and mean wave height are used to characterize the coastal morphology type (Fig. 1). Although such classifications are useful for comparing different types of inlets in a wide variety of coastal settings, or to explain processes at inlets that have insufficient data, there is a risk of over generalization. In an elaboration on the Hayes (1979) work, Davis and Hayes (1984) already conclude that a wide range of wave and tidal conditions can produce coastal configurations with similar appearances.

In this paper, we will demonstrate that in Ameland Inlet, a mixed-energy wave-dominated inlet according to the Hayes (1979) classification, parts of the ebb-tidal delta in which the processes are distinctively tide dominated or wave dominated can be observed. This dominance is controlled by the local distribution of the channels and shoals of the ebb-tidal delta. Moreover, we document the fundamental morphological changes that took place in less than two decades and which comprise a significant change in both size and orientation of the main ebb channel. Our analysis is based on sixteen bathymetric surveys of the inlet-ebb delta system collected between 2005 and 2021 and an extensive dataset of hydrodynamic observations collected in 2017. As part of the regular coastal monitoring program, Rijkswaterstaat, the Dutch water management authority, surveys the ebb-tidal delta in 3-year intervals. Additional yearly surveys were collected between 2007 and 2010 in the framework of a coastal safety study (project SBW-Waddenzee; Zijderveld and Peters, 2006). Between 2016 and 2020, half-yearly bathymetric surveys of the ebb-tidal delta were collected as part of the Kustgenese 2.0 (KG2) project. Carried out in anticipation of a pilot nourishment on the ebb-tidal delta, the KG2 project also included an extensive field campaign in Ameland inlet (in Dutch Amelander ZeeGat: AZG) between August 29, 2017 and October 09, 2017 in which hydrodynamic measurements were carried out and samples of sediment and benthic fauna were collected in a variety of locations covering the ebb-tidal delta and tidal basin (Van Prooijen et al., 2020; Van der Werf et al., 2019). As a result, a dataset of unprecedentedly high spatial and temporal resolution for the entire ebb-tidal delta and adjacent coastlines is available for analysis. Our goal is to combine the information and compile a synthesis of the morphodynamics of Ameland Inlet and the resulting shoreline changes, to provide a basis for present day and future management of the coasts of the Wadden islands bounding Ameland inlet.

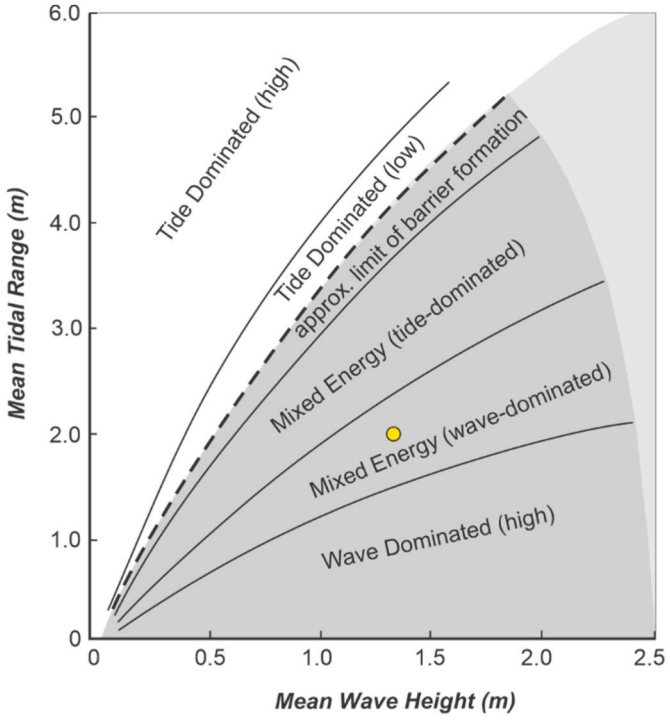

Fig. 1. General relationships between tidal range and wave height as it relates to coastal morphology (modified after Davis and Hayes, 1984). Yellow dot represents Ameland Inlet, the Netherlands.

2. Ameland Inlet and ebb-tidal delta

Ameland Inlet is centrally located in the chain of Dutch Wadden Islands. With a mean tidal range of nearly 2 m and an annual average significant wave height of 1.4 m, it can be classified as a mixed-energy wave-dominated inlet (Fig. 1). However, the morphology of the ebb-tidal delta shows tide-dominated characteristics such as a large ebb-tidal delta and deep main channel (Fig. 2). An eastward longshore transport dominates along the barrier island coasts as a result of the prevailing wind and waves out of the westerly quadrants. Estimates of the longshore drift vary considerably. Along the updrift (in relation to the principal direction of littoral transport) coastline of Terschelling island, alongshore transports of 0.5–0.6 to 1.0 million m^3/year were reported by Tanczos et al. (2000) and Spanhoff et al. (1997), respectively. Ridderinkhof et al. (2016) estimates the longshore drift rate to range between 0.3 and 0.5 million m^3/year along the eastern, downdrift part of the Terschelling coast and 0.8–1.2 million m^3/year along the Ameland coast.

Fig. 2 provides a detailed overview of the main channels and shoals that form the present day (2021) Ameland Inlet. In the inlet throat, between the islands of Terschelling and Ameland, a deep main ebb channel exists along the west coast of Ameland (Borndiep). The deepest parts of the channel exceed 25 m in depth. The associated Ameland tidal basin has a length of about 30 km and covers an area of 270 km^2. Approximately 60% of the basin area consists of intertidal shoals (Eysink, 1993). In the basin, Borndiep connects to Dantziggat that curves eastward into the basin towards the Pinkewad, a topographic high (tidal divide, or watershed) separating the basin from its neighbor. To the west, separated by the shoal Zeehondenplaat, a smaller channel system is formed by Oosterom, Boschgat and Blauwe Balg, all curving southward towards the tidal divide of Terschelling (Terschellinger Wad). A shallow platform dissected by a series of small, dynamic channels, Boschplaat, is present between the eastern island tip of Terschelling and Borndiep.

The main ebb channel (Borndiep-Akkepollegat) has had a pronounced northward outflow onto the ebb-tidal delta in the past (Fig. 3, 2005–2017), but relocated to a westward position around 2017. This new westward outflow is called Nieuwe Akkepollegat. An updrift orientation of the main ebb channel is observed along many of the larger Wadden Sea inlets and related to the interaction of the marine shore-parallel tidal currents and the inlet currents that dominates over waves (Sha, 1989).

Two dominant features on the ebb-tidal delta are the ebb chutes that have formed along its western margin. The oldest and most seaward ebb chute and its associated lobe (hereafter called Kofmansplaat) now covers most of the shoal area known as Kofmansbult. To the north the (pilot) ebb-delta nourishment is still visible as a shallow platform just seaward of the Kofmansbult. Eastward migration of the Kofmansplaat has distorted the outflow of Akkepollegat and rotated the channel eastwards. Extensive sedimentation has occurred in the distal part of the Akkepollegat, and in the 2021 bathymetry the channel is hardly visible.

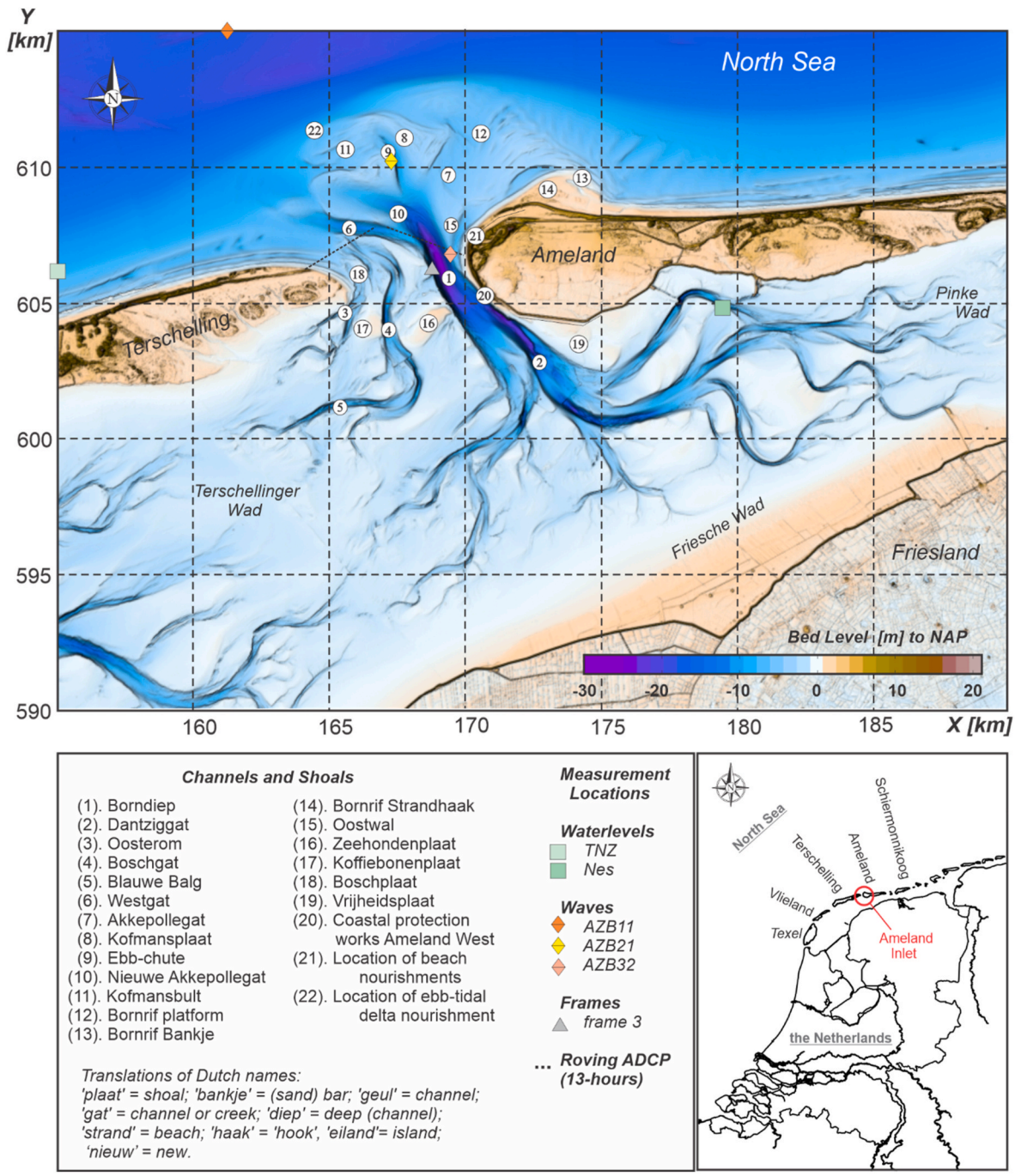

Fig. 2. Overview of the channels and shoals that form the present day Ameland Inlet. The underlying DEM is based on the 2021 Vaklodingen for the ebb-tidal delta and 2017 measurements of the basin. Bed level is measured with respect to NAP (Normaal Amsterdamse Peil) datum, approximately mean sea level.

The main ebb-tidal delta shoal area lies eastward of Akkepollegat, which is downdrift in relation to the principal direction of the longshore transports. This large shoal area or swash platform is named Bornrif. On the present day platform clear swash bars are not present on the central part of the shoal, but a series of large bedforms (sand waves) propagate over the platform towards the coast (Brakenhoff et al., 2019). Bar migration did occur between 2005 and 2017 as the shoal Bornrif Bankje formed and propagated along the north-eastern margin of the ebb-tidal delta towards the coast of Ameland. Bornrif Bankje attached to the coast in 2017 just east of the Bornrif Strandhaak. The Bornrif Strandhaak is a former ebb-delta shoal that attached to the coastline around 1985 (Elias et al., 2019). This shoal merger constitutes a natural mega nourishment that compares to the man-made "Sand motor", a 20 million m^3 sand nourishment along the Holland coast (Stive et al., 2013) both in dimension and layout, and has supplied the (downdrift) coastline of Ameland with sand over the past decades. Just to the west of this location, at the northwest tip of Ameland Island, repeated nourishments and extensive shore protection works are needed to maintain the coastline. A large nourishment is visible in the 2019 bathymetry, as 2.8 million m^3 of sand was placed along the coastline. While shoal attachments built out the coastline of Ameland, the opposite was observed along the coastline of Terschelling. The eastern tip of this island has retreated over 1.5 km since 1975 (Elias et al., 2019; Elias, 2021).

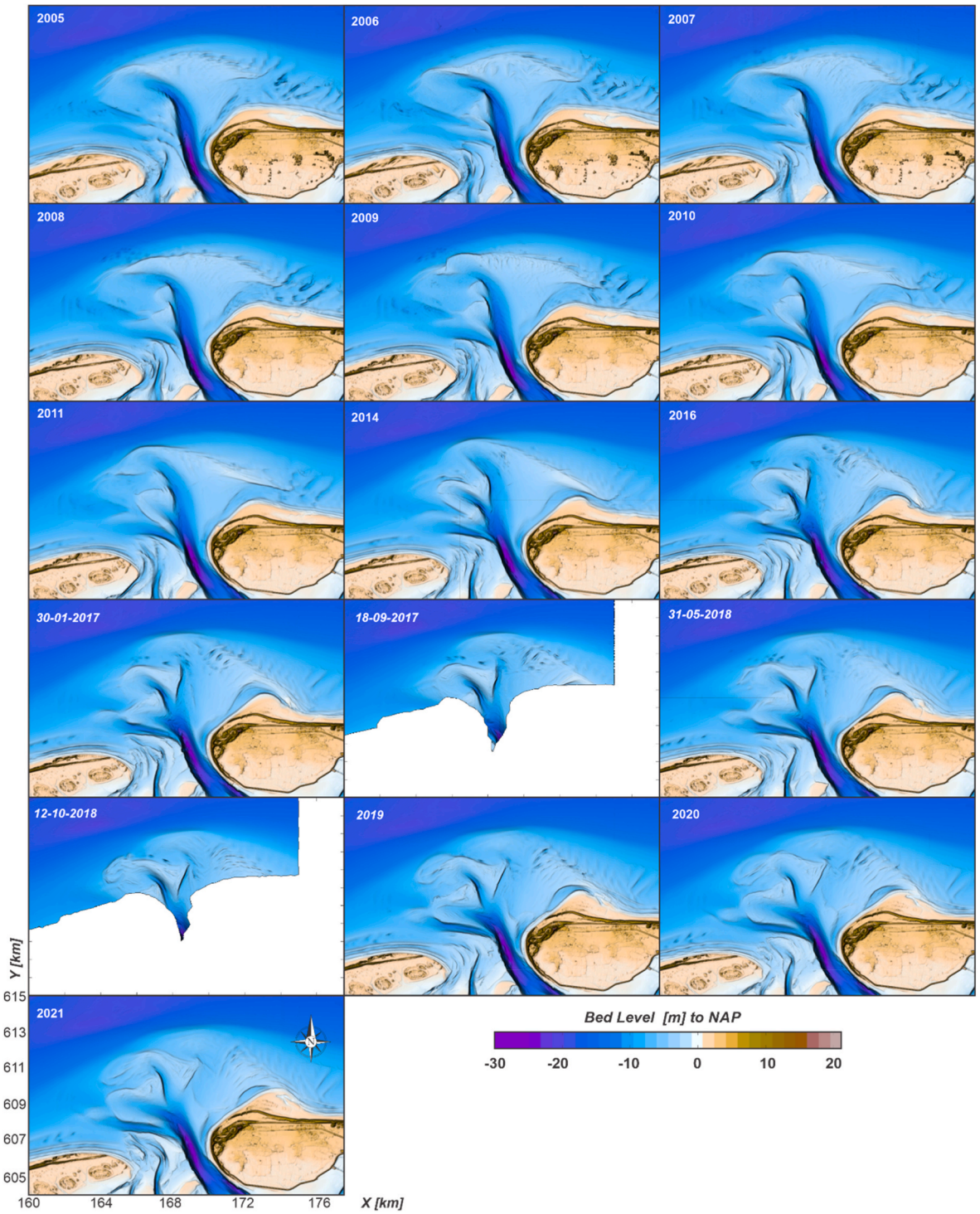

Fig. 3. Bathymetric maps illustrating the evolution of the channels and shoals on the Ameland ebb-tidal delta between 2005 and 2021.

3. Field observations

3.1. Seabed composition

3.1.1. Grain sizes

The median grain size (d_{50}) of Ameland ebb-tidal delta sediment is very homogeneous, with 79% of samples between 170 and 230 μm (Fig. 4a). Sediment fines in a clockwise direction ($\theta \rightarrow$from -90° to 45°) and further from the inlet. The variance in d_{50} also decreases steadily in a clockwise direction and with distance from the inlet (ρ). The coarsest samples tend to be found in deeper channel areas near the inlet, where tidal currents are persistently strong (>=1 m/s). The mud content is <1% for 81% of samples, and the only samples with >1% mud content are located in deeper channel areas and the distal edge of the ebb-tidal delta (Fig. 4b). The mud within samples from the channel consists of lumps of consolidated clay that were eroded from older deposits and transported as bed load. Conversely, mud in the distal samples was likely freshly deposited after Storm Sebastian, several days prior to their collection. Pearson et al. (2021a) demonstrated that mud is regularly found in suspension over the sandy bed of the delta, even if it does not

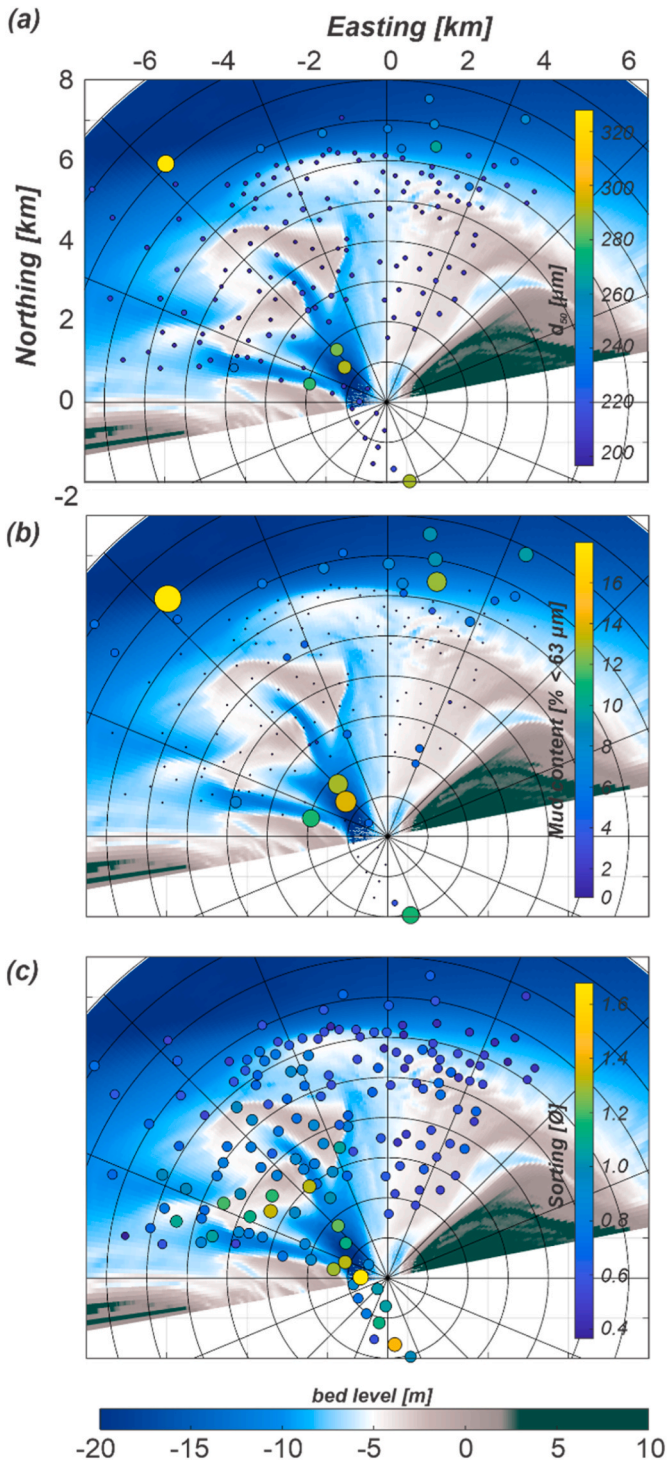

Fig. 4. (a) Overview of the median grain size (d_{50}), (b) mud content in the bed (defined as sediment <63 µm) and (c) sediment sorting.

deposit there.

There is no trend in sorting with either ρ or θ, but 80% of samples are well sorted ($0.35 < \sigma < 0.5$ based on the Logarithmic Folk and Ward graphical measure (Blott and Pye, 2001). Moderately sorted samples ($0.5 < \sigma < 1$) tend to be located on the distal edge of the delta, while the most poorly sorted samples ($\sigma > 1$) are mainly found in the channels (Fig. 4c). The body of the ebb-tidal delta is overwhelmingly well-sorted fine sand.

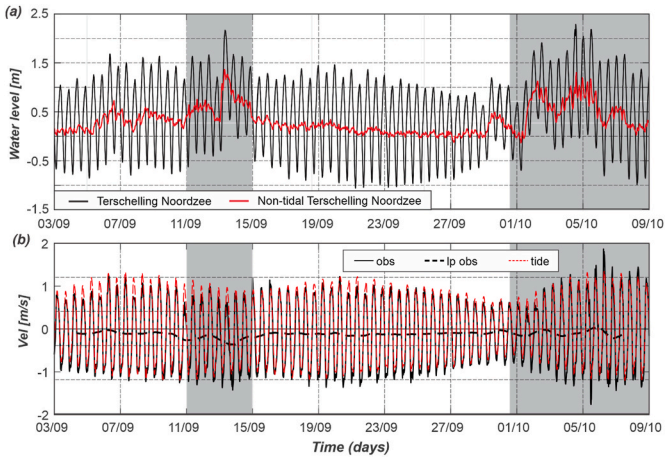

Fig. 5. (a) Measured water levels during the AZG campaign at station Terschelling Noordzee. Red line illustrates the (non-tidal) setup derived through tidal analysis of the data. (b). An overview of the depth-averaged velocities and low-pass filtered velocities in Borndiep (frame 3). Positive velocities are directed into the Wadden Sea and negative velocities towards the North Sea. Station locations are shown in Fig. 2. Grey areas indicate elevated water levels related to storm Sebastian (11–15 September 2017) and Storm Xavier (30 September – 9 October).

3.1.2. *Interpretation*

These observations may be explained by breaking waves, which promote sorting of the sand by the continuous resuspension, resulting in well-sorted deposits on the distal (wave-dominated) portion of the ebb delta. Pearson et al. (2021b; this issue) demonstrated clear signs of grain size-selective transport on the ebb delta via a pre-nourishment tracer study in 2017. In channels, all sizes are transported, from clay flocs to stones, and finer fractions settle on slack tide. These may get buried under new deposits, resulting in poor sorting there.

3.2. *Tides and tidal flow*

Along the Wadden Sea coast, tides are semi diurnal and propagate from west to east. The mean tidal range increases from 1.4 m at Den Helder to 2.0 m at Ameland inlet and continues to increase even further in eastward direction. The tidal range increases to 3 m during spring tide and drops to around 1.5 m during neap tide. During major storm events, the rise in water level due to reduced air pressure and wind-generated setup can exceed 1.5 m. For example, during the AZG campaign an increase exceeding 1 m was observed offshore during the storm events of September 11– September 15, 2017 (Storm Sebastian) and Storm Xavier that started on September 30, 2017 (Fig. 3). In the basin, setup levels were even larger. Setup gradients can drive complicated residual flow fields over the complex bathymetry of the Wadden Sea, and generate shore-parallel velocities and throughflow between adjacent basins (Duran-Matute et al., 2014; van Weerdenburg et al., 2021; this issue). The increased volume of water stored in the Wadden Sea due to the larger setup can considerably enhance the outflow velocities in the inlets following the storm events, thereby affecting channel dimensions, the ebb-tidal delta development, and adjacent beaches (Koch and Niemeyer, 1978; Krögel, 1995; Elias and van der Spek, 2006).

3.2.1. *Inlet flow velocities*

An estimate of the (tidal) flow velocities in the inlet throat can be obtained from Frame 3, placed in the main channel Borndiep near its western slope at a depth of −20 m NAP. An upward looking ADCP, mounted near the top of the frame at a height of about 2.3 m above the seabed, recorded time-series of velocity profiles at 1 Hz intervals throughout the deployment. Depth-averaged velocities were calculated from the measured velocity profile by fitting a log distribution. The tidal

modulation dominates the velocity signal and shows a strong influence of the spring-neap variation (Fig. 4b). During spring tide, peak velocities exceed 1.35 m/s and reduce to around 0.50 m/s during neap tides. On average, ebb velocities at this location exceed the flood velocities. The contributions of the tidal and non-tidal components in the velocity fields can be estimated through low-pass filtering of the data (Fig. 4b, dashed line). The non-tidal signal averages of −0.12 m/s over the recorded timeseries. During the 2 storm events, non-tidal flows are considerably larger and exceed −0.2 m/s. The negative value indicates a net outflow, which confirms the statement that residual net outflow is likely related to meteorological forcing (van Weerdenburg et al., 2021; this issue).

3.2.2. Drifter observations

Lagrangian surface currents were measured using drifters equipped with GPS trackers. Positioning of the drifters were recorded at 1 Hz intervals using an internal logger. The drifters were designed as floating devices that follow the top layer velocities but are minimally influenced by wind. The main experiments were carried out in a series of experiments around Frame 4 and 5, at the location of the planned nourishment (De Wit et al., 2018). In this section, we will use the results of a single large-scale experiment conducted on September 9, 2017. The goal of this experiment was to better understand the spatial variations in velocity on the ebb-tidal delta scale circulation patterns and flow pathways. During this experiment drifters were released and retrieved after a full tidal cycle. From these experiments, velocity magnitudes and directions were determined.

Fig. 6 illustrates the resulting drifter pathways. Based on a series of numerical tracer experiments, Elias (2017) hypothesizes that Westgat forms a transition area on the ebb-tidal delta. Particles located landward of Westgat mostly exchange with the southern part of the domain, while particles to the north exchange with Borndiep and are transported back onto the ebb-tidal delta. The drifter experiment confirms this hypothesis for surface currents. All drifters deployed along the Terschelling coast follow the Boschgat channels into the basin. Drifters that are picked up by Borndiep are transported seaward into the ebb chutes or through Akkepollegat onto the ebb-tidal delta. These patterns may differ for sediment travelling along or near the bed, but still provide an additional line of evidence to explain likely suspended sediment pathways.

3.2.3. Ebb and flood volumes

The tidal motion is known to drive a significant flow through the inlet throat. In the past, measurements of the discharge have been taken frequently in transects across the inlet throat (Borndiep) by roving 13-h ship measurements (Van Sijp, 1989; Barsingerhorn et al., 2003; Briek et al., 2003; Studiedienst Hoorn, 1973). On average, ebb and flood volumes through the inlet are c. 400–500 million m^3. The residual

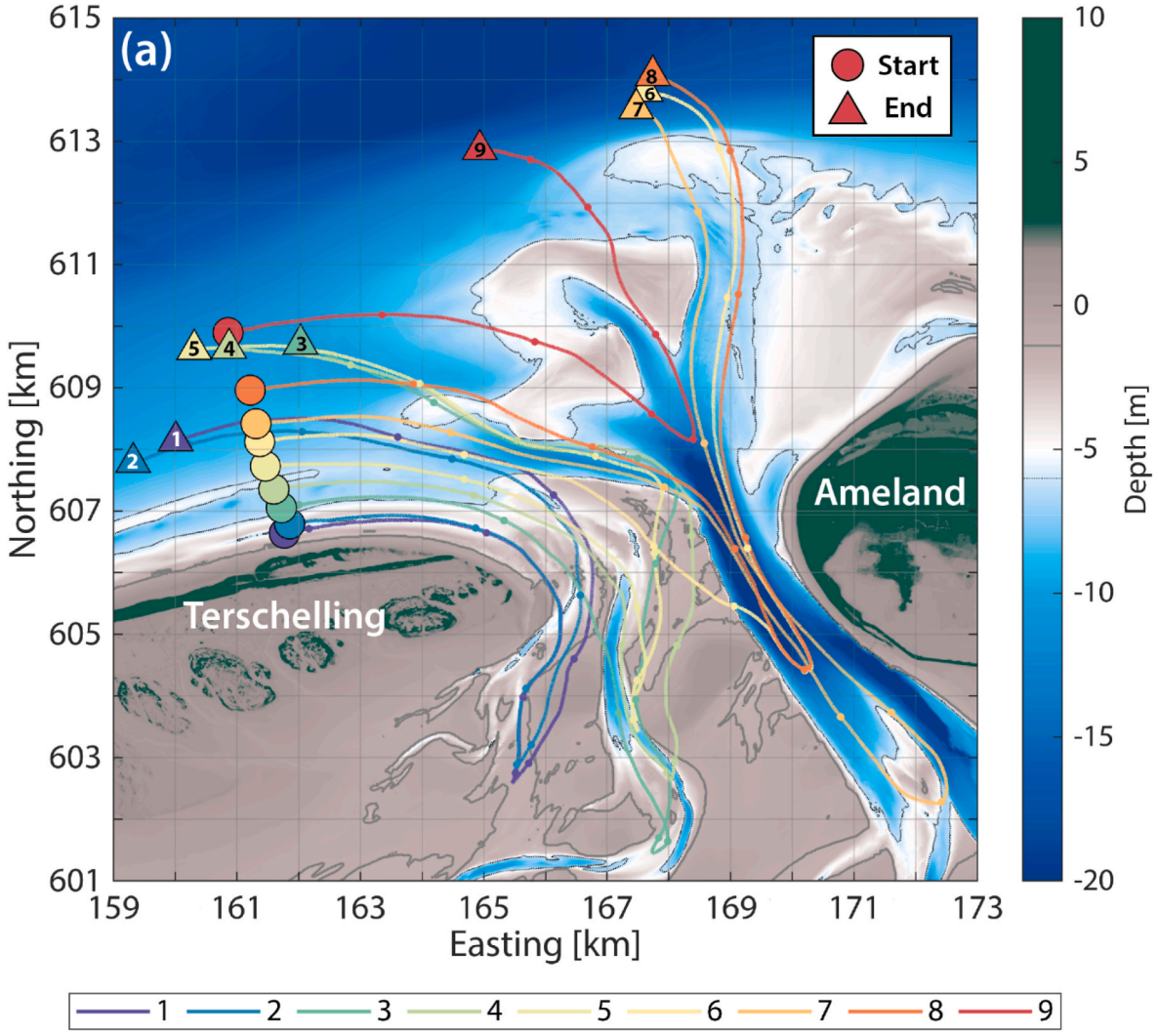

Fig. 6. Lagrangian flow (drifter) measurements. (a) GPS tracks of the large-scale deployment on September 9th, 2017 during spring tide. Drifters were deployed in a 3 km long line north of Terschelling at flood tide (circles) and retrieved at different locations around the inlet at ebb tide (triangles). Small dots along the drifter paths indicate position every hour from 9:00 until they were retrieved.

discharges are small, less than 10% of the gross ebb and flood volumes. No clear preference in residual discharge dominance could be observed as half of the measurements were flood dominant and the other half ebb dominant (Table 1).

During the AZG campaign, roving ADCP measurements were obtained along 2 transects just seaward of the inlet. The transects were sailed simultaneously by two survey vessels over a 13-h time frame. Together, these two surveys provide an estimate of the total flow through the inlet. Raw ADCP data were transformed to global coordinates using heading and tilt information supplied by the vessel. Velocity measurements were corrected to remove the motion of the vessel using the bottom ping, which estimates the vessel speed with respect to the seabed. The experiments were conducted during three distinct phases of the tide. Measurement 1 was taken on September 1, 2017 during neap tide. As a result, the ebb and flood volumes were smaller compared to the measurements taken at an average tide (September 5, 2017) or spring tide (September 19, 2017). All measurements show a small net flow that varied from ebb dominance during neap tide and flood dominance during the other 2 experiments. Although the discharges were not recomputed to a mean discharge, they are of similar magnitude to the measurements taken during previous campaigns (Table 1).

The important conclusion from these experiments is that, despite significant changes in the basin and ebb-tidal delta bathymetry, discharges through the inlet have not changed considerably. Present day values of gross and net flow are in line with the older measurements. Secondly, the ebb and flood volumes are in near equilibrium, which results in a relatively small net tidal residual. With no clear ebb or flood dominance, the net ebb or flood dominant flow in the inlet may depend on the phasing in the tide and especially the prevailing meteorological conditions. Similar conclusions were drawn in the modelling studies of Duran Matute et al. (2014), and Van Weerdenburg et al. (2021; this issue).

3.3. Wave observations

3.3.1. Wave climate 2007–2017

Analysis of the wave records over the 2007–2017 timeframe reveal that the significant wave height remains below 2 m and is wind generated. During storms, wave heights occasionally reach values between 4.5 and 9.1 m (less than 1% of the record). The dominant wind and wave directions differ considerably (Fig. 6). The largest and most frequent winds occur from the southwest (225°), a direction hardly present in the wave record due to the sheltering of the mainland and the barrier islands (Fig. 7). Roughly 33% of the wave directions lie between west-southwest and north-northwest (235°–305°). Most waves (62%) are from directions between north-northwest and east (305°–90°). The remaining 4% are offshore directed and do not significantly contribute to sediment transport. Wave periods ($T_{1/3}$) typically vary between 3 and 6 s for lower wave conditions (89% of the measurements). For typical storm waves (H_{sig} = 2–3 m) a mean wave period of 6.0 s occurs, increasing to 7.6 s for severe storms (H_{sig} > 4 m). Contributions of swell are minor. Wave periods over 9 s are only measured occasionally (0.1% of the record). The short-wave periods indicate that the wave climate is dominated by wind waves generated in the North Sea basin.

3.3.2. Field campaign 2017

During the AZG campaign, a mix of calm and stormy conditions was encountered (Fig. 8). Through the majority of the campaign wind velocities were below 10 m/s with wind directions mostly from southerly to westerly directions (180°–270°; Fig. 8a). Corresponding wave heights are small, below 1 m, with wave periods of 4 s or less. During Storm Sebastian (11–15 September 2017) windspeeds peaked at a velocity of 20 m/s from an on average westerly direction, and the wave height reached 6 m at the buoy located just seaward of Ameland (Buoy AZB11). This peak wave height is not representative for the entire storm event as waves mostly remained below 3 m. This storm event was followed by a relative calm period until the second storm event started on September 30, 2017 (Storm Xavier). The second storm event is less severe in maximum wind speeds. However, wind velocities of around 10 m/s from a west – northwesterly direction were sustained over a 5-day period. As a result, a prolonged period of 3–4 m wave heights was measured at the offshore buoy (AZB11; Fig. 8b).

In general, the shallow ebb-tidal delta is considered to act as a natural breakwater for the adjacent shorelines and to prohibit wave propagation from the North Sea into the basin effectively. Refraction and wave breaking on the shoals (especially during the high wave-energy events with large morphodynamic impact) and wave blocking by the supra-tidal shoal areas modify and distort the nearshore wave climate (e.g. Hine, 1975; FitzGerald, 1988; Elias and Hansen, 2013). A comparison of the wave heights for buoys AZB11 (located just offshore of Ameland inlet), station AZB21 (located in the distal part of Akkepollegat), and station AZB32 (in the nearshore ebb-tidal delta just south of Westgat) partly confirms these statements (Fig. 8b). Wave heights at station AZB21 are noticeably smaller compared to AZB11. Waves that exceed approximately 2 m in height break on the ebb-delta front. Only limited additional dissipation of wave energy occurs between station AZB21 and AZB32. This is due to the short distance and presence of the relatively deep channel between the two stations.

A noticeable feature in the timeseries of stations AZB21 and AZB32 is the strong tidal modulation in wave height (Fig. 8b). The correlation between the peak in ebb flow and the peak in wave heights suggests that this modulation is likely related to wave-current interaction. The importance of wave-current interactions in wave height amplification was also studied by Elias et al. (2012) on the ebb-tidal delta of the Columbia River. Based on measurements and process-based models, these authors concluded that waves near-doubled in the Columbia River during opposing ebb-tides. Water level variations are likely important here as well. A comparison of the low-pass filtered wave heights and low-pass filtered water levels (Fig. 8c) shows a correlation of larger wave heights during higher water levels. Since wave heights and surge both correlate to the wind velocity, this is not proof that water levels cause the higher wave heights, but it is at least an indication that higher waves generally coincide with a higher water level over the ebb-tidal delta.

Table 1
Overview of measured ebb and flood volumes in Borndiep.

Survey year	dates	Measured Discharge [10^6 m^3]			Mean Discharge [10^6 m^3]		
		Flood	Ebb	Net	Flood	Ebb	Net
1937	–	–	–	–	406	−431	−25
1968–1973	109 flood tides 110 ebb tides	–	–	–	518	−494	24
1996		502	−450	52	448	−395	53
1999	26-10-1999 04:00–18:00	542	−573	−31	416	−454	−38
2001	22-01-2001 05:30–18:30	557	−547	10	407	−418	−11
2017 (1)	01-09-2019 05:00–18:00	330	−339	−9			
2017 (2)	05-09-2019 05:00–18:00	480	−449	31			
2017 (3)	19:09–2019 05:00–18:00	545	−506	39			

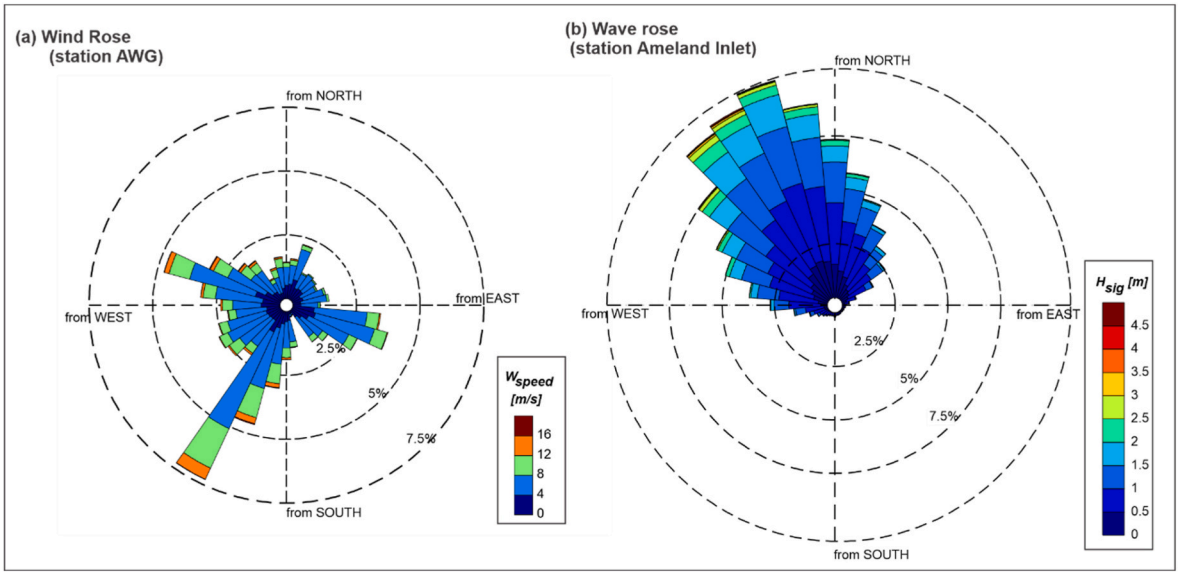

Fig. 7. Overview of the (a) wind and (b) wave conditions representative for Ameland Inlet based on data over the timeframe 2007–2017.

4. Morphodynamics of the ebb-tidal delta

4.1. Channel and shoal dynamics

Between 2005 and 2021, large morphodynamic changes have occurred on the ebb-tidal delta. The abundant sediment supply from longshore transport and the continuous erosion of the island Terschelling contributed to the formation of a large linear bar flanking the westside of Borndiep (Figs. 3 and 9, transects B, C). As this bar grew in size and extended seaward, small instabilities started to develop. These instabilities triggered the formation of a series of initially small ebb chutes ending in crescent-shaped lobes (Fig. 3, 2006, 2008, 2014), which eventually led to complete relocation of the main channels and shoals on the ebb-tidal delta (Elias et al., 2019).

The 2005 bathymetry is dominated by a single main central channel (Fig. 3), which has a northward orientation in the inlet, but curves northwesterly on the ebb-tidal delta due to the large Bornrif shoal and the preferential hydraulic gradient (Sha, 1989). The bulk of the ebb delta deposits are present in the main shoal area Bornrif, located east of the main channel. Along the two island shorelines, smaller flood-dominated channels occur (Westgat and Oostgat). No distinct flood channel is observed in the inlet throat, but a shallow platform occurs between the tip of Terschelling Island (Boschplaat) and the Borndiep channel. In the inlet, Borndiep retains a stable position and depth (Fig. 9, transect A). The Boschgat platform is dissected by a series of small channels that connect the western part of the basin with the North Sea. These channels are highly mobile and do not exceed a depth of 7 m. Since 1975 substantial erosion occurred at Boschplaat and the island tip has retreated over 1.5 km westward. This retreat is clearly visible in Fig. 9, Transect A. The erosion is linked to the eastward retreat of an ebb-tidal shoal that historically sheltered Boschplaat (Elias et al., 2019). In the absence of this shoal, waves can propagate relatively undisturbed towards the coast. This means that wave breaking-induced transport along the Terschelling coast can induce significant coastal erosion and eastward transport towards Borndiep.

Between 2005 and 2006, a first ebb chute emerged as a small channel just north of Westgat (Fig. 3). As this channel grew, it pushed sediment seaward, forming a small sand lobe on top of the Kofmansbult shoal. By 2008, a second ebb chute and lobe had formed to its south, overwhelming the first system. In total, the ebb chute migrated over 3 km across the ebb-tidal delta with rates varying between 160 m/year and 500 m/year (Fig. 3). By 2014 the lobes of the first and second ebb chute merged, forming a large shoal just west of Akkepollegat. The sedimentation on the Kofmansbult continued to dominate the morphodynamic changes of the central-downdrift ebb-delta platform. A pronounced sand lobe grew and pushed forward, rotating clockwise. By 2016, the ebb lobe (now called Kofmansplaat) covered the major part of the Kofmansbult. This large shoal increasingly constricted flow in the neighboring Akkepollegat. This channel subsequently reduced in size and was deflected downdrift, to the east. As a result, by 2016 a downdrift-curved channel remained. Using the −10 m contour as a proxy for channel displacement, we can observe a nearly 1.3 km eastward displacement of the end of Akkepollegat. It is probable that the terminal lobe deposits in front of the channel were transported to the east, because a large shallow shoal (Bornrif Bankje) continued to grow along the north-eastern margin of the ebb-delta shoal during this period.

Sandwiched between Westgat and the second ebb chute, a new (third) ebb chute started to form between 2011 and 2014, This new ebb chute quickly grew and expanded to the (north)west. An ebb lobe formed as a shallow shoal extending up to a depth of 4 m, that propagated over the underlying platform located at −7 m (Fig. 9, transect C). The outbuilding of the sand lobe is characterized by a steep seaward slope, which is characteristic of outbuilding due to transport by the ebb tide (Buonaiuto and Kraus, 2003) and can be observed at other Wadden Sea inlets as well (e.g., Texel inlet, Elias and van der Spek, 2017). The −10 m contour migrated nearly 900 m westward between 2011 and 2016. While the shallower part of the Akkepollegat channel primarily rotated eastward (up to the −10 m contour), the deepest part significantly reduced in length; over 300 m between 2005 and 2009. As flow in Akkepollegat became increasingly restricted, a new outlet for Borndiep was needed. While the distal part of Akkepollegat rotated clockwise (to the east), the proximal part, towards the inlet throat, rotated anti clockwise and is now (in 2020) connected directly to the third ebb-chute channel. This channel (Nieuwe Akkepollegat) has taken over as new main ebb-channel. This relocation of the Akkepollegat ebb channel is an example of the ebb-tidal delta breaching model of sand bypassing (FitzGerald, 1988; FitzGerald et al., 2000), although the details differ from the original model (see Discussion below).

Progradation of the front of the ebb lobe and increased erosion of the ebb-chute channel during winter may be related to wind-driven storm surge and additional exchange over the watersheds during (westerly) storm conditions. In the North Sea, a close correlation between wind speed and wave height occurs. In the winter season large storms and strong winds occur that not only generate the large waves, but also result

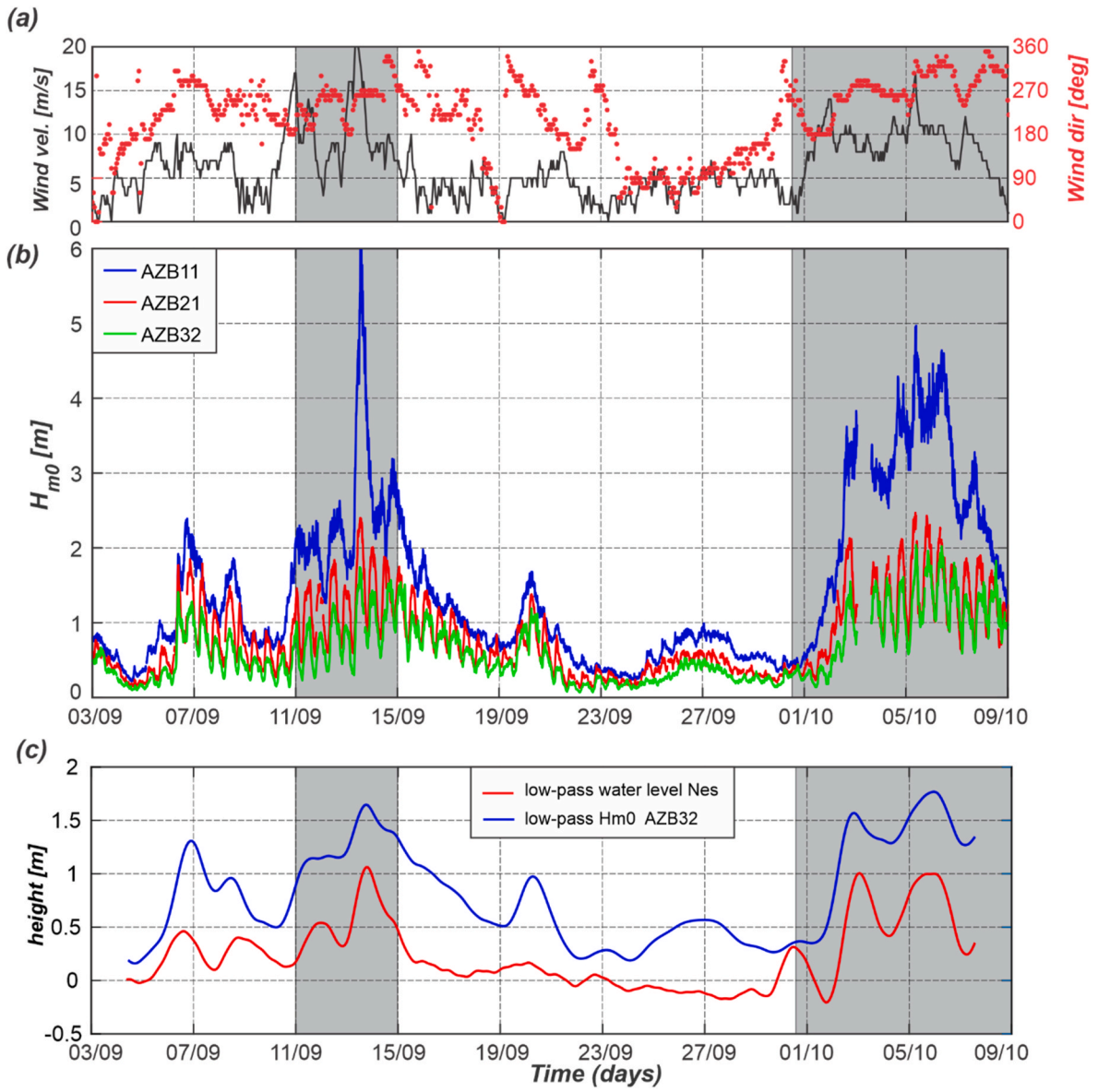

Fig. 8. (a) Wind speed and direction observed at the KNMI station of Terschelling (b).Wave heights observed at the Amelander Zeegat stations AZB11, AZB21 and AZB32. (c) Low-pass filtered water levels (Nes) and wave heights for buoy AZB32. See Fig. 2 for locations. Grey areas indicate elevated levels due to storm Sebastian and Storm Xavier.

in large-scale surge (Fig. 5a). This surge can significantly increase the exchange of flow through the inlet (van Weerdenburg et al., 2021; this issue). As the basin drains, the ebb velocities may be considerably increased, resulting in strong velocities over the ebb-tidal delta and increased migration of the ebb-chute and ebb-lobe systems. These findings raise questions of our general conceptual models describing tidal inlet systems. These systems seem to be in equilibrium under more-or-less average conditions, but are distorted during more energetic conditions.

Large changes were also observed on the Bornrif platform, which occupies the eastern half of the ebb-tidal delta (Fig. 9, transects B, F, G). Although the basal part of the Bornrif platform remains in place, the formation, migration, and eventual merger of Bornrif Bankje dominated the developments between 2011 and 2020. The origin of Bornrif Bankje can be traced back to the 1989–1999 timeframe. During this period the northern ebb-delta front showed a large outbuilding and increase in shoal height at the seaward end of Akkepollegat (Fig. 9 transect F). This outbuilding continued until 2011. It is likely that wave-breaking on this shallow shoal area resulted in downdrift sand transport along the ebb-tidal delta margin, and Bornrif Bankje slowly started to emerge on the north-east side of the ebb-tidal delta (2008–2010). The shoal continued to migrate eastward and landward (2011–2014) at a rate between 150 and 430 m/year (based on the −5.0 m contour). By 2014, only a small channel remained between the Bornrif Strandhaak and Bornrif Bankje. This migration is likely due to a combination of wave-driven and tidal sand transport, amplified by flow contraction and acceleration of the along-hore North-Sea tides around the steep slope of the delta. The tip of Bornrif Bankje attached to the Ameland coastline in 2018, just downdrift of the Strandhaak (Fig. 9, transect G). At the location of this transect the Strandhaak has eroded over 350 m since 2005.

4.2. Sediment budget

Estimates of transport rates on the ebb-tidal delta are obtained by quantitative analysis of sedimentation-erosion patterns derived by subtracting the 2005 bathymetry from the 2021 bathymetry (Fig. 10a). The interaction of tidal, wind and wave-driven flow with the complex ebb-tidal delta bathymetry produces a convoluted pattern of mutually

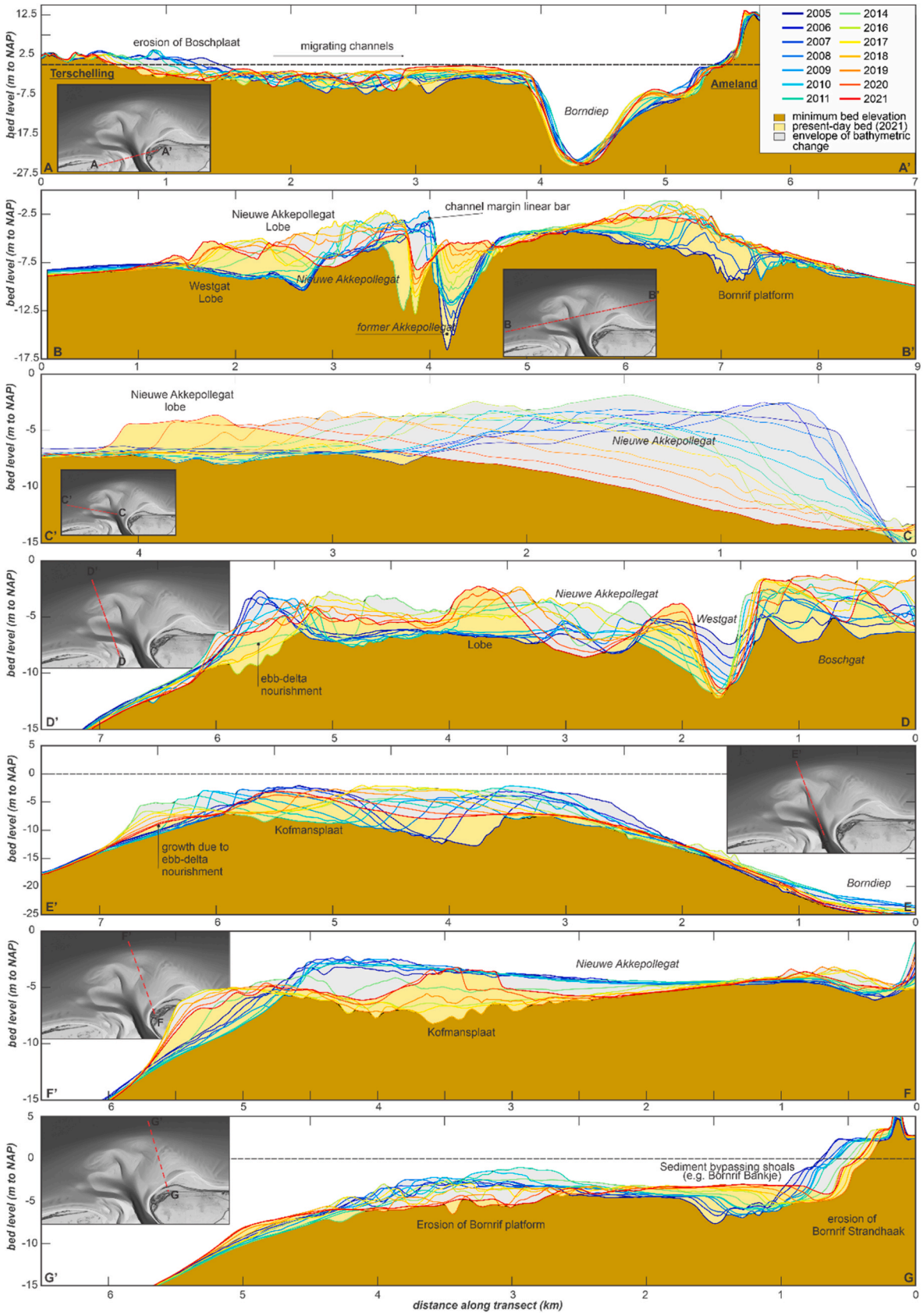

Fig. 9. Morphological development of the ebb-tidal delta between 2005 and 2020, illustrated by a series of bathymetric transects (see inset for locations).

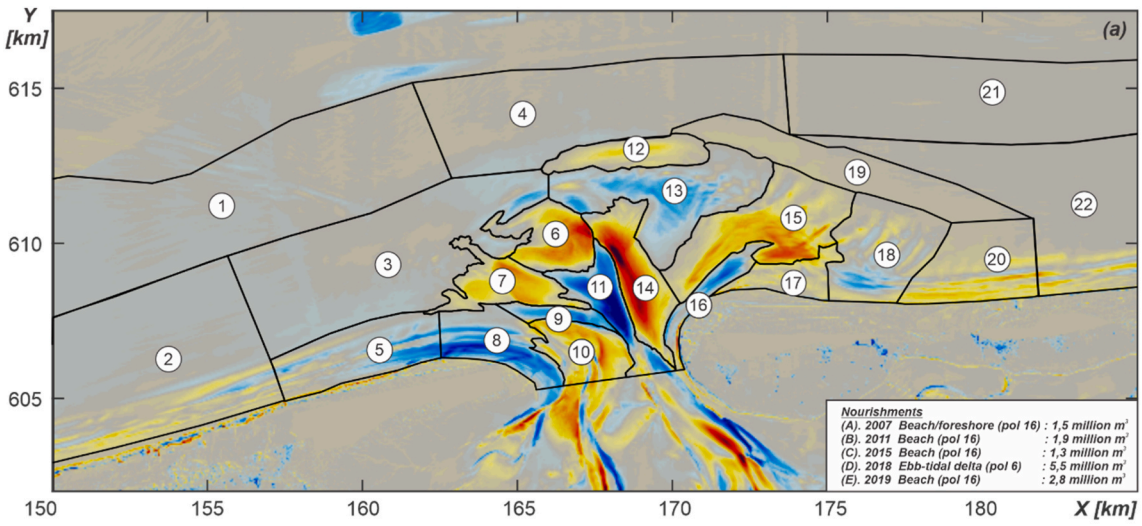

	Polygon	dV [10⁶m³]
Kofmansbult	3	-9.0
Boschplaat	5	-5.7
	8	-6.7
Ebb-lobes	6	11.6
	7	8.7
Westgat	9	-3.4
Boschgat	10	8.3
Ebb-chutes	11	-17.3
Akkepollegat	14	23.1
Bornrif	12	3.5
	13	-13.7
	15	19.8
	16	-2.0
	17	0.9
	18	-1.5
	19	1.5
Total ETD		18.3
Terschelling coast	1	1.2
	2	0.6
Ameland coast	4	-3.2
	20	5.8
	21	-1.2
	22	1.6
Total coast		4.8

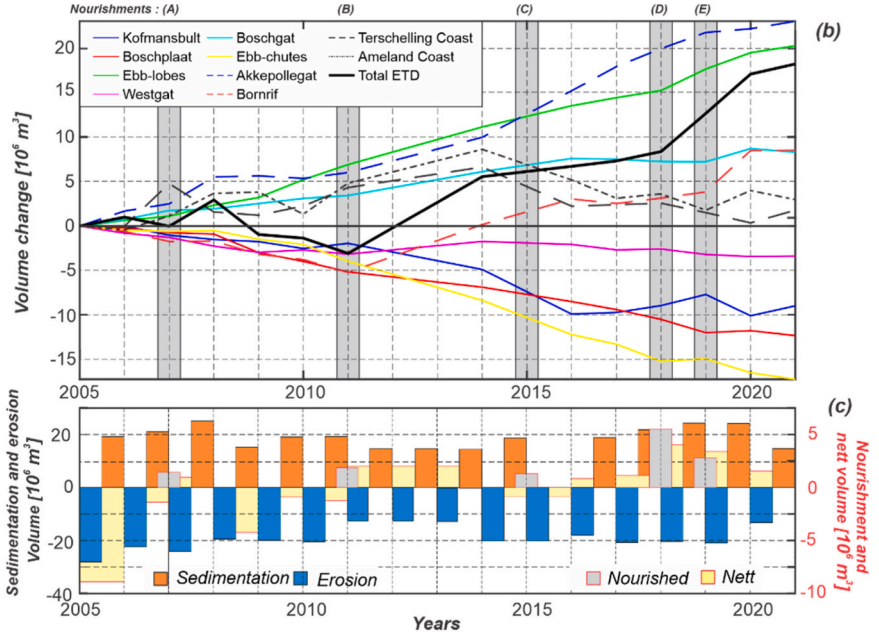

Fig. 10. A summary of the sedimentation-erosion patterns and volume changes of the ebb-tidal delta between 2005 and 2021. (a). Bed-level change map between 2005 and 2021. Polygons indicate the morphological domains that were used in the volumetric analysis. Along the barrier islands the mean high waterline is used as cut-off value in the computations. (b) Timeseries of volumetric (net) change for each of the domains since 2005. The grey shading illustrates the nourishments that were executed along the Ameland coastline and on the ebb-tidal delta. (c) Yearly net and gross sedimentation and erosion volumes for the ebb-tidal delta and volume of nourishments.

linked sedimentation-erosion areas. Between 2005 and 2011 a small sediment loss, −0.5 million m^3/year, occurs, while between 2011 and 2021 the net sediment gain equals 2.0 million m^3/year. In total a net volume gain of the ebb-tidal delta of 18.3 million m^3 is observed between 2005 and 2021. This increase is small given that averaged gross volumetric change equals 47 million m^3/year (Fig. 10c). Part of the volume gain may be related to sand nourishments as between 2005 and 2021 7.5 million m^3 of sand was placed on the eroding coastline on NW Ameland (Fig. 10, [polygon 16]) and 5.5 million m^3 directly on the ebb-tidal delta.

Major erosion areas include the Boschplaat [5,8], the Westgat and ebb-chute channels [9,11] and the seaward part of Bornrif [13]. The island tip of Terschelling, Boschplaat shows a continuous severe erosion with a total sediment loss of 12.4 million m^3 between 2005 and 2021. Part of this material (8.3 million m^3) was deposited in the shallow area between Boschplaat and Borndiep. Major sediment accumulation, 11.6 million m^3 and 8.7 million m^3 is also observed in the two ebb lobes [6 and 7]. Part of the deposits originate from the formation and scouring of the ebb chutes (channels) [11] which resulted in a net erosion of 17.3 million m^3. In addition, 5.5 million m^3 of sand was placed directly on the Kofmansplaat [6] in the form of a pilot nourishment.

The seaward part of Bornrif is erosive (13.7 million m^3 [13]). Most of this sediment likely accreted landward in the shoal areas just offshore of Ameland, (19.8 million m^3, [15]). Large sedimentation was also observed along the eastern margin of the main ebb channel (23.1 million m^3 [14]). A small area of accretion, 3.5 million m^3, occurs on the western tip of the ebb-delta front [12]. This area formed as Akkepollegat rotated eastward and temporarily formed a near straight channel with Borndiep. As a result, it pushed the edge of the ebb-tidal delta seaward. This material now lies outside the active part of the ebb-tidal delta.

For a limited, seaward, part of the domain the measurements allow for the reconstruction of the half-yearly volume changes for the years 2018 and 2019 and we can get insight in the difference in response between summer and winter conditions (see Elias et al., 2020). These

measurements illustrate that the infilling of Akkepollegat [14] mainly occurs during winter conditions. Over the winter timeframe the net sedimentation equals 2.0–2.2 million m^3, while in the summer season the volume gain reduces to 0.2–0.7 million m^3. It is likely that the increased wave action during these stormy months pushes more sediments landward, from the ebb-delta platform into the ebb channel. A similar response, albeit smaller in magnitude, is observed on the Bornrif platform [13]. Here the erosion rate of 1.0–1.4 million m^3 during the winter periods exceeds the observed erosion of 0.2–0.3 million m^3 during summer.

4.3. Synthesis of decadal-scale ebb-tidal delta evolution

The observed morphodynamic changes over the period 2005–2021 show that the ebb-tidal delta can be subdivided in several zones that are governed by a specific combinations of underlying steering processes and that show typical morphodynamic behavior (Fig. 11, zone I–VI).

Zone I – Updrift coastline; The longshore transports along the coastline of Terschelling and the continuous erosion of the Boschplaat supply sediment to the inlet system and its surroundings. Both waves and tides play an important role here. Nearshore waves generate a net eastward flow and stir up sediments that can be transported by the flood tidal flow. These transports feed the sub-tidal platform that is present between Westgat and Boschgat. Earlier studies (e.g., Elias, 2017) hypothesized that part of this erosion is related to increased wave exposure, as the present day ebb-tidal delta directly offshore Boschplaat is relatively deep. This allows waves to propagate far into the inlet throat, introducing an eastward, wave-driven transport along the Terschelling coast and into the inlet (Boschgat area).

Zone II – Sub-tidal platform; The sub-tidal platform, the shallow area between Westgat, Boschplaat and Borndiep, is a mixed-energy environment wherein both tides and waves are important. The bathymetry shows large variability in the position, size and extend of smaller-scale channels. Tidally driven transports through these smaller channels transport sediments into the south-western part of the back-barrier basin. Wave-driven transports result in an eastward net sediment movement towards and into the main channel (Borndiep).

Zone III – Dynamic ebb-delta platform; The western, central part of the ebb-tidal delta is highly dynamic and in essence dominated by tidal flow in the central part and by waves on the seaward shoals. At this location the formation, growth, and migration of ebb chute and lobe systems dominate the morphodynamic changes. The steep bed-slope gradients on the seaward side of the sand lobes indicate that lobe outbuilding results from tide-driven sediment supply from the ebb chutes. Wave breaking and related sediment transports on these shallow shoals drive sediments landward and eastward. As a result, the ebb shoals not only prograde seaward but also migrate eastward, and the bulk of the sediment in the delta is contained in the downdrift side of the shoal. The ebb lobe outbuilding into Akkepollegat constrained the flow (and related transports) even further. As a result, the deep central part of Borndiep now connects directly to the southernmost ebb chute. The most recent (2021) bathymetry shows that this chute has transformed into the main ebb channel that has for a major part taken over the role of the Akkepollegat.

The continuous growth of the southern ebb lobe may result in complete closure of the northern ebb chute and the merger of the two sand lobes. This would form a large shoal area in the central part of the ebb-tidal delta. A secondary effect of the abandonment of Akkepollegat is the infilling of the former channel. Especially along the western margin of the Bornrif platform, we observe a large depositional area. This area is fed by the wave-driven transports over the Bornrif platform (*Zone V*), and by the ebb currents.

Zone IV – ebb-tidal-delta margin. The ebb-delta margin is usually not considered as a separate element. However, both the hydrodynamic and the morphodynamic observations indicate that the processes here are slightly different from the shallower parts of the delta, and that they are

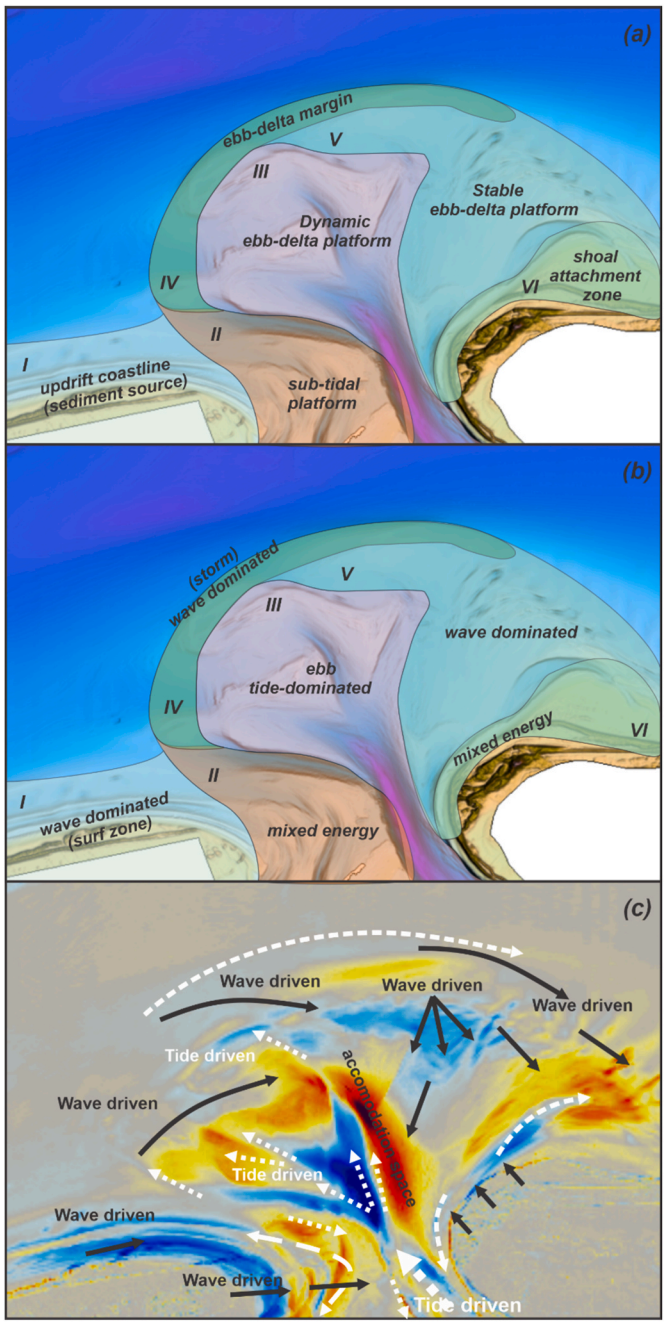

Fig. 11. Conceptual description of the recent morphodynamic behavior of the ebb-tidal delta.

dominated by storm wave conditions. During most of the year, shoals accumulate on the ebb-delta platform. These shoals form an equilibrium between low wave energy and tidal energy. During storms, the largest waves break on these shoals, which results in large fluxes of sediments towards the east. As a result, large pulses of sediment episodically feed the Bornrif platform and contribute to the sediment accumulation here. A volume analysis of the morphodynamic changes shows that sediment accumulation in winter significantly exceeds the summer accumulation. Apart from the storm events, this part of the ebb delta is relatively inactive as it is too deep for waves to break under normal conditions. The dominant transport mechanisms here are then the alongshore tidal currents that accelerate as the flow contracts around the ebb delta.

Zone V – Stable ebb-delta platform (main shoal area); The main shoal area Bornrif is located downdrift of the main channel. The shoal built out

seaward when Akkepollegat was still the main ebb channel, which resulted in sediment accumulation ~1 km seaward of the current position of the ebb delta margin. This accumulation was a balance between the seaward ebb transports and the landward wave-driven transports. As tide-transported sediments primarily accumulate on the western, updrift, margin of the ebb-tidal delta, the distal part of the Bornrif platform is sediment starved. With Akkepollegat now largely abandoned, landward wave-driven transports prevail, and net erosion is observed at the delta front. These sediments are transported landward and accumulate in shoal deposits on the Bornrif platform, just seaward of the Ameland coast.

Although it seems contradictory, the landward sediment transport temporarily induces increased erosion of the island coastline. This is a commonly observed phenomenon (e.g., Gaudiano and Kana, 2001) and related to the constriction and contraction of (flood) flow between the coastline and advancing swash bars. Typically, the residual ebb velocity is dominant in the main channel, while residual flood velocities occur on either side of the channel along the island coastlines. As the advancing swash bar grows in height, it constricts and traps the flow between the bar and the coast. As a result, a channel forms directly along the coastline that not only increases coastline erosion, but also slows the advance of the swash bar. Sediments are transported along the coast by the tidal currents in the channel, and accumulate in the shoals that form on either side. Depending on the sediment supply, these shoals can grow to such dimensions that they overwhelm the channel and episodically attach to the coastline (e.g., Bornrif Strandhaak). Alternatively, they temporarily grow and finally dissipate when sediment supply reduces or stops due to larger-scale changes on the ebb-tidal delta. *Zone VI* describes this shoal attachment zone.

Zone VI – Shoal attachment zone; The shoal attachment zone is a net accretional area. The present day shoreline, the large bulbous outcrop, shows the remnants of the Bornrif Strandhaak, a former ebb-tidal delta shoal that attached to the coast in 1985. With the attachment of the Strandhaak, the coastline migrated seaward by 1.5 km. This was followed by a retreat of over 500 m as the deposits were subsequently reworked and predominantly transported downdrift, feeding the adjacent coast of Ameland (Elias et al., 2019). A new shoal attachment occurred in 2017 as the Bornrif Bankje attached to the coastline at the tip of the Bornrif Strandhaak. In contrast to the previous two attachments that occurred on the north-western tip of Ameland near Borndiep, this recent attachment occurred further downdrift at the ebb-delta margin.

Based on the above-described zones, we can summarize the net sand fluxes in the inlet and ebb-tidal delta (Fig. 11c). Waves erode the updrift island tip, the sand is transported to the east. Part of the sand is delivered to the back-barrier basin, whereas part of the sand ends up in Borndiep channel and is transported onto the ebb-tidal delta by ebb currents. The sand is deposited in the prograding lobes of ebb-dominated channels, both large and small. Breaking waves force these sandy shoals to the east, thereby pushing the ebb channels in the same direction and onto the ebb-delta platform. The ebb-delta platform accumulates sand, that is transported to the downdrift island in the form of swash bars. These swash bars merge with the island shoreline, thus feeding the island with sand.

5. Interpretation and discussion

The relocation of the main ebb channel on the ebb-tidal delta of Ameland Inlet is an example of the ebb-delta breaching model of sand bypassing (FitzGerald et al., 2000), although the time scale involved is much longer. In the original publication, the breaching process is described as occurring gradually within a year time or catastrophically during a storm. In the Ameland case, it took the formation of three successive ebb chutes and lobes between 2005 and 2019 to establish a new, updrift-directed connection for the main ebb channel. The large dimension of Ameland Inlet and its ebb-tidal delta are the likely cause for the longer duration of process. On the other hand, during this period swash bars formed, migrated onshore and attached to the downdrift island, simultaneously with the breaching process. Readjustment of the delta geometry formed during preceding stages and migration followed by reworking of the ebb lobes supplied the sand for swash bar formation. Fig. 3 shows the changes in configuration of the delta platform and Ameland shoreline between 2010 and 2021.

5.1. Waves and tides

According to the general classification based on the wave versus tidal energy relation postulated by Davis and Hayes (1984), Ameland inlet is a typical mixed-energy, wave-dominated system (see Fig. 1). As our observations show, the ebb-tidal delta contains distinct areas that are wave or tide-dominated. These areas are not fixed, but evolve with the changing morphodynamics of the ebb delta. Even though the wave energy and tidal range does not change between 2005 and 2021, one can argue that the 2005 ebb-tidal delta shows tide-dominated characteristics: a deep main channel and an ebb-tidal delta that is large and extends far seaward (Figs. 3 and 2005). Between 2005 and 2021 the bathymetry shows more-and-more wave-dominated characteristics. The main ebb channel is abandoned and reforms in a westward position, the terminal lobe of the ebb-delta is pushed landward and large, shallow shoals migrate over the ebb-delta platform. These shoals are part of the sediment bypassing sequence in which sediment is transported over the ebb-delta platform from the updrift to the downdrift barrier island. Our detailed and frequent bathymetric observations illustrate that the sediment bypassing process consists of different stages where wave or tide dominance spatially varies.

A notable sediment bypassing sequence starts between 2005 and 2006, when small instabilities or distortions occur on the channel-margin linear bar that flanks the main ebb channel. Prior to formation of these instabilities, the sediment bypassing sequence starts with the formation of this large elongated bar due to sediment delivery from the updrift Terschelling coastline. This could be due to the lack of wave sheltering by the ebb-tidal delta. Detailed measurements of the wave heights over the ebb-tidal delta illustrate that the wave sheltering effect of the ebb-tidal delta is limited (Fig. 8). Even with the extensive shallow shoal areas present in 2017 (Fig. 3 and 2017) wave breaking on the ebb-tidal delta is limited to waves that roughly exceed 2 m in height. Such conditions only occur during moderate to severe wave conditions. During most of the time, waves can propagate undisturbed to the adjacent coastlines.

In the 2005 configuration of the ebb-tidal delta, the main ebb-channel extends far seaward and as a result, the main shoals are located seaward and to the north of Terschelling. Along the Terschelling coast, waves can propagate undisturbed towards the coast and far into the inlet. Both the coastline and the Boschgat region (the shallow area between the island tip and Borndiep channel) are wave dominated. Wave-driven transports can thus effectively transport sediment away from the Terschelling coast into the main channel. These sediments are then redistributed into the basin and seaward onto the ebb-tidal delta, where they accumulate in shoals flanking the main channel.

In 2005 this shoal reached a volume and position that became unstable. The mechanisms behind the formation of this instability are not completely clear, but likely it is tide dominated. Located near the confluence of several channels, flows in this area are characterized by strong horizontal shear. Some of the morphodynamic instabilities dampened out, but others grew and transformed into small ebb chute-like channels (Figs. 3, 2005 and 2006), with ebb lobes forming seaward of the chutes. Between 2006 and 2016, three major ebb-chutes developed. These channels rapidly grew and migrated seaward along the updrift embankment of the main channel (2006–2011). Not all these systems remained stable, but by 2016, two well-established ebb-chute and ebb-lobe systems formed. As the ebb chutes migrated seaward away from the inlet, tides became less important and the wave-dominated transports (west to east) started to dominate on the ebb lobes. As a

result, the seaward migration rate reduced and the ebb lobes became increasingly asymmetric, with largest shoal volume downdrift of the ebb chute. Subsequent downdrift migration of the ebb-chute and lobe increasingly impacted and constrained the flow in the main ebb channel. Eventually the constrained flow in the main ebb channel resulted in the formation of a new westward-directed outflow from the main ebb channel (Figs. 3, 2019 and 2020). Based on these observations, we argue that the central part of the ebb-tidal delta transformed from a tide-dominated to a wave-dominated setting.

Large-scale channel and shoal migrations are not observed on the downdrift platform. During the entire timeframe a large, shallow platform was retained. Sediment delivery from this platform to the coast did however alter considerably. With a tide-dominated main ebb channel (situation 2005) sediments accumulate in front of this channel, far seaward on the terminal lobe of the ebb-tidal delta and a relatively high shoal forms here. Contraction of the east-west tidal currents result in a net eastward tidal transport along the terminal lobe, which is augmented by wave-driven transports during storm conditions. As a result, the shoal propagates along the margin of the ebb-tidal delta and attaches onto the Ameland coast, far eastward of the island tip. To the west, only limited sediment supply occurs, and this area is sediment starved.

5.2. Management of ebb-tidal delta shorelines

The extensive ebb-tidal deltas along the barrier islands of the Wadden Sea play an important, arguably dominant role, in the evolution of the adjacent barrier island coastlines (FitzGerald et al., 1984; Sha, 1989; Wang et al., 2012; Elias and van der Spek, 2017; Elias et al., 2019). This statement is clearly demonstrated by the responses of the islands tips adjacent to Ameland Inlet (as presented in this study). The updrift island tip (Terschelling) has retreated over 1.5 km since 1975, while repeated shoal attachments built out the downdrift coastline of Ameland. However, the bypassing of large volumes of sand from the updrift to the downdrift island takes several years to decades and cause coastal management dilemmas at shorter time scales. At the northwest tip of Ameland inlet, over 7.5 million m^3 of sand was nourished since 2005 (see summary in Fig. 10) based on the coastal hold-the-line policy in the Netherlands (see e.g., Hillen and de Haan, 1993; Hillen and Roelse 1995 for more information). From a morphodynamic viewpoint, the placement of this amount of sand at the island tip may be somewhat surprising, as this area forms the endpoint of the shoal bypassing cycle, and frequent shoal attachments have historically built out this part of Ameland (Cheung et al., 2007; Israël and Dunsbergen, 1999; Elias et al., 2019). Typically, a large (several km), near-instantaneous, seaward relocation of the coastline occurs after attachment (e.g., the Bornrif Strandhaak in 1985), but this is followed by many years to decades of retreat as the attached deposits are reworked.

As described above, the most recent shoal attachment occurred far eastward of the island tip. With limited sediment supply to the west, and flow contraction around the island tip, sustained large-scale erosion is observed. This erosion can only be reversed if the shoal attachment zone migrates westward. Although we cannot predict the future, the present day configuration of the ebb-tidal delta shows that such a process is presently occurring. The terminal lobe no longer shelters the Bornrif from wave energy, so increased landward (wave-driven) transport occurs on the Bornrif platform. These sediments contribute to shoal accumulation just seaward of the Ameland coast (Fig. 2, Oostwal shoal). In addition, large lobes are present in the central part of the ebb-tidal delta that may migrate landward.

An opposite development is observed at the island tip of Terschelling. Along the inhabited, central part of Terschelling island, a reference coastline was defined and will be maintained via nourishments (which has not been necessary until present). However, the uninhabited island tip has a nature reserve status, which means that no coastal maintenance occurs. Natural processes were allowed to continue, resulting in an over 1.5 km retreat of the island tip since 1975.

If the coastal maintenance policy is aimed at preservation of the coastline position, e.g. through a yearly evaluation, this means that the understanding of the natural system needs to be on a similar level. In the ebb-tidal delta system, this means understanding the intra-delta dynamics (the behavior of the individual shoals and channels). As demonstrated in this study, the intra-delta dynamics of an ebb-tidal delta are complex and can change drastically through time. Our observations show that depending on intra-delta dynamics, small changes in the sediment-bypassing sequence determine the maintenance needs of the adjacent barrier islands. Detailed measurements and observations are needed to unravel all the intricate interactions that take place.

The ebb-tidal delta is commonly generalized as a large reservoir of sand (Kraus, 2000). The volume of this reservoir is shown to relate to the tidal prism of the inlet and as such is related to the dimension of the back-barrier basin, which makes sense as larger tidal prisms can build out and sustain larger ebb-tidal deltas. This study shows that the ebb-tidal delta of Ameland Inlet, and likely the other ebb-tidal deltas along the Wadden Sea, function as sand reservoir for the downdrift barrier island. The delta is much less likely to act as a sand reservoir for the back-barrier basin, since only a limited amount of the sand volume eroded from the updrift island of Terschelling is transported into the basin.

For successful and sustainable management of the barrier islands a thorough understanding of the ebb-tidal dynamics and its interaction with the adjacent barriers is of utmost importance. Such understanding requires detailed observations and interpretations of the changes of smaller-scale features such as the individual channels and shoals.

6. Concluding remarks

This paper reports the analysis of a dataset of sixteen bathymetric surveys of the Ameland Inlet and its ebb-tidal delta collected between 2005 and 2021, supported by an extensive dataset of hydrodynamic observations collected in 2017. The information is compiled into a synthesis of the morphodynamics of Ameland Inlet and its neighboring shorelines, to provide a basis for present day and future coastal management.

Between 2005 and 2021, large morphodynamic changes have occurred on the ebb-tidal delta. The abundant sediment supply from longshore transport and the continuous erosion of the updrift island Terschelling contributed to the formation of a large linear bar flanking the westside of the main ebb channel Borndiep. As this bar grew in size and extended seaward, small instabilities started to develop. These instabilities triggered the formation of a series of ebb chutes and lobes, that eventually led to complete relocation of the main channels and shoals on the ebb-tidal delta.

The observed morphodynamic changes show that the ebb-tidal delta can be subdivided in several zones that show typical morphodynamic behavior. Based on these zones, we can summarize the net sand fluxes in the inlet and ebb-tidal delta. Waves erode the updrift island tip, the sand is transported to the east. Part of the eroded sand volume is transported into the back-barrier basin, the other part of the sand volume ends up in the main ebb channel in the inlet and is transported onto the ebb-tidal delta. The sand is deposited in the prograding lobes of ebb-dominated channels, both large and small. Breaking waves force these sandy shoals to the east, thereby pushing the ebb channels in the same direction and onto the ebb-delta platform. The ebb-delta platform accumulates sand that is transported to the downdrift island in the form of swash bars. These swash bars merge with the island shoreline, thus feeding the island with sand.

The relocation of the main ebb channel on the ebb-tidal delta of Ameland Inlet is an example of the ebb-delta breaching model of sand bypassing, although the time scale involved is much longer. At Ameland Inlet, it took the formation of three successive ebb chutes and lobes between 2005 and 2019 to establish a new, updrift-directed connection for the main ebb channel. The large dimension of Ameland Inlet and its

ebb-tidal delta are the likely cause for the longer duration of process. During this period, swash bars formed, migrated onshore and attached to the downdrift island, simultaneously with the breaching process.

Our observations show that the smaller-scale dynamics of the ebb-tidal delta are complex and can change drastically through time. The limited wave-sheltering by the ebb-tidal delta exposes the shorelines of the adjacent barrier islands to significant wave-driven sand transports that necessitated repeated sand nourishments under the Dutch coastal maintenance policy.

The study confirms that the ebb-tidal delta of Ameland Inlet acts as a sand reservoir for the downdrift barrier island. The delta sand body is not a reservoir for the back-barrier basin, since the basin is predominantly supplied with sand eroded from the updrift island of Terschelling. This knowledge is essential for strategic nourishment of either the adjacent coasts or the basin and for predicting long-term responses to sea-level rise.

Declaration of competing interest

The authors declare that they have no known competing financial interests or personal relationships that could have appeared to influence the work reported in this paper.

Acknowledgments

The paper summarizes the results of research conducted as part of the projects: KPP Beheer en Onderhoud Kust and Kustgenese 2.0. Both projects aim to improve our understanding of the evolution of the Dutch coast and tidal inlets which is the basis for effective coastal management in the Netherlands. Harry de Looff and Marian Lazar (both Rijkswaterstaat Traffic and Water management) are thanked for pleasant collaboration, advice, and assistance in obtaining the datasets presented here. The comments of the reviewers greatly improved the manuscript and are much appreciated. Stuart Pearson is funded by the research programme 'Collaboration Program Water' with project number 14489 (SEAWAD), which is (partly) financed by NWO Domain Applied and Engineering Sciences.

Open access to the Vaklodingen is provided by Deltares at: https://svn.oss.deltares.nl/repos/openearthrawdata/trunk/rijkswaterstaat/vaklodingen/

Open access to the Kustgenese 2.0 data is provided at https://doi.org/10.4121/collection:kustgenese2 or can be requested from Rijkswaterstaat at https://waterinfo-extra.rws.nl.

References

Barsingerhorn, S., Briek, J., Huizinga, M.A., Hut, J., Noordstra, P., 2003. Meting Bornrif/Borndiep September 1996. Project Strobodi. Report 98.006 (In Dutch). Rijkswaterstaat, directie Noord-Nederland, Delftzijl.

Blott, S.J., Pye, K., 2001. GRADISTAT: a grain size distribution and statistics package for the analysis of unconsolidated sediments. Earth Surf. Process. Landforms 26 (11), 1237–1248.

Brakenhoff, L., Ruessink, G., van der Vegt, M., 2019. Characteristics of saw-tooth bars on the ebb-tidal deltas of the Wadden Islands. Ocean Dynam. 69 (11), 1273–1285. https://doi.org/10.1007/s10236-019-01315-w.

Briek, J., Huizinga, M.A., Hut, J., 2003. Stroommeting Zeegat Van Ameland 2001. Report 2003-169 (In Dutch). Rijkswaterstaat, Directie Noord-Nederland, Delftzijl.

Bruun, P., Gerritsen, F., 1960. Stability of Coastal Inlets. North-Holland Publishing Company, Amsterdam, the Netherlands.

Buonaiuto, F.S., Kraus, N.C., 2003. Limiting slopes and depths at ebb-tidal shoals. Coast. Eng. 48 (1), 51–65. https://doi.org/10.1016/S0378-3839(02)00160-6.

Cheung, K.F., Gerritsen, F., Cleveringa, J., 2007. Morphodynamics and sand bypassing at Ameland inlet, The Netherlands. J. Coast Res. 23 (1), 106–118. https://doi.org/10.2112/04-0403.1.

Davis, R.A., Hayes, M.O., 1984. What is a wave-dominated coast? Mar. Geol. 60, 313–329.

De Wit, F.P., Tissier, M.F.S., Pearson, S.G., Radermacher, M., van de Ven, M.J.P., van Langevelde, A.P., Vos, T.A., Reniers, A.J.H.M., 2018. Measuring the Spatial and Temporal Variability of Currents on Ameland Ebb-Tidal Delta. NCK Days Conference. Haarlem, the Netherlands. March 23 2018.

Dean, R.G., 1988. Sediment interaction at modified coastal inlets: processes and policies. In: Aubrey, D., Weishar, L. (Eds.), Hydrodynamics and Sediment Dynamics of Tidal Inlets. Lecture Notes on Coastal and Estuarine Studies 29. Springer, New York, pp. 412–439.

Duran-Matute, M., Gerkema, T., de Boer, G.J., Nauw, J.J., Gräwe, U., 2014. Residual circulation and freshwater transport in the Dutch Wadden Sea: a numerical modelling study. Ocean Sci. 10 (4), 611–632. https://doi.org/10.5194/osd-11-197-2014.

Elias, E.P.L., 2017. Stroming en sedimenttransport langs de Boschplaat, Terschelling. Report. Deltares, Delft.

Elias, E.P.L., 2021. De morfologische ontwikkeling van de Boschplaat – Terschelling. Report 11205236-003. Deltares, Delft, p. 49.

Elias, E.P.L., Hansen, J.E., 2013. Understanding processes controlling sediment transports at the mouth of a highly energetic inlet system (San Francisco Bay, CA). Mar. Geol. 345, 207–220.

Elias, E.P.L., van der Spek, A.J.F., 2006. Long-term morphodynamic evolution of Texel Inlet and its ebb-tidal delta (The Netherlands). Mar. Geol. 225, 5–21. https://doi.org/10.1016/j.margeo.2005.09.008.

Elias, E.P.L., van der Spek, A.J.F., 2017. Dynamic preservation of Texel Inlet, The Netherlands: understanding the interaction of an ebb-tidal delta with its adjacent coast. Neth. J. Geosci. 96 (4), 293–317. https://doi.org/10.1017/njg.2017.34.

Elias, E.P.L., Gelfenbaum, G., van der Westhuijsen, A.J., 2012. Validation of a coupled wave-flow model in a high-energy setting: the mouth of the Columbia River. J. Geophys. Res. 117, C09011. https://doi.org/10.1029/2012JC008105.

Elias, E.P.L., van der Spek, A.J.F., Pearson, S., Cleveringa, J., 2019. Understanding sediment bypassing processes through analysis of high-frequency observations of Ameland Inlet, The Netherlands. Mar. Geol. 415, 105956. https://doi.org/10.1016/j.margeo.2019.06.001.

Elias, E.P.L., van der Spek, A.J.F., Pearson, S., 2020. Understanding the Morphological Processes at Ameland Inlet. Kustgenese 2.0 Synthesis of the Tidal Inlet Research, Report 1220339-008-ZKS-008. Deltares, Delft, p. 82.

Eysink, W.D., 1993. Impact of sea level rise on the morphology of the Wadden Sea in the scope of its ecological function. General considerations on hydraulic conditions, sediment transports, sand balance, bed composition and impact of sea level rise on tidal flats. In: Report ISOS*2, Project Phase 4. Rijkswaterstaat. National Institute for Coastal and Marine Management RIKZ, The Hague.

FitzGerald, D.M., 1988. Shoreline erosional-depositional processes associated with tidal inlets. In: Aubrey, D., Weishar, L. (Eds.), Hydrodynamics and Sediment Dynamics of Tidal Inlets. Lecture Notes on Coastal and Estuarine Studies 29. Springer, New York, pp. 186–225.

FitzGerald, D.M., 1996. Geomorphic variability and morphologic and sedimentologic controls on tidal inlets. In: Mehta, A.J. (Ed.), Understanding Physical Processes at Tidal Inlets Based on Contributions by Panel on Scoping Field and Laboratory Investigations in Coastal Inlet Research. Journal of Coastal Research SI 23, pp. 47–71.

FitzGerald, D.M., Penland, S., Nummedal, D., 1984. Control of barrier island shape by inlet sediment bypassing: east Friesian Islands, West Germany. Mar. Geol. 60 (1–4), 355–376.

FitzGerald, D.M., Kraus, N.C., Hands, E.B., 2000. Natural mechanisms of sediment bypassing at tidal inlets. In: Technical Note ERDC/CHL CHETN-IV-30. US Army Corps of Engineers, Vicksburg, MS, USA.

Gaudiano, D.J., Kana, T.W., 2001. Shoal bypassing in mixed energy inlets: geomorphic variables and empirical predictions for nine South Carolina inlets. J. Coast Res. 280–291.

Hayes, M.O., 1975. Morphology of sand accumulation in estuaries: an introduction to the symposium. In: Cronin, L.E. (Ed.), Estuarine Research, vol. 2. Academic Press, New York, pp. 3–22.

Hayes, M.O., 1979. Barrier Island morphology as a function of tidal and wave regime. In: Leatherman, S.P. (Ed.), Barrier Islands: from the Gulf of St Lawrence to the Gulf of Mexico. Academic Press, New York, pp. 1–27.

Hayes, M.O., FitzGerald, D.M., 2013. Origin, evolution, and classification of tidal inlets. In: Kana, T., Michel, J., Voulgaris, G. (Eds.), Symposium in Applied Coastal Geomorphology to Honor Miles O. Hayes. Journal of Coastal Research SI, 69, pp. 14–33. https://doi.org/10.2112/SI_69_3.

Hillen, R., de Haan, Tj, 1993. Development and implementation of the coastal defense policy for The Netherlands. In: Hillen, R., Verhagen, H.J. (Eds.), Coastlines of the Southern North Sea. American Society of Civil Engineers, New York, NY), pp. 118–201.

Hillen, R., Roelse, P., 1995. Dynamic preservation of the coastline in The Netherlands. J. Coast Conserv. 1 (1), 17–28.

Hine, A.C., 1975. Bedform distribution and migration patterns on tidal deltas in the Chatham Harbor Estuary, Cape Cod, Massachusetts. Estuar. Res. 2, 235–253.

Hoorn, Studiedienst, 1973. De Waterbeweging in Het Borndiep. Rijkswaterstaat, Studiedienst Hoorn. Report 73.3 (in Dutch).

Hubbard, D.K., Oertel, G., Nummedal, D., 1979. The role of waves and tidal currents in the development of tidal-inlet sedimentary structures and sand body geometry: examples from North Carolina, South Carolina and Georgia. J. Sediment. Petrol. 49, 1073–1092.

Israël, C.G., Dunsbergen, D.W., 1999. Cyclic morphological development of the Ameland inlet, The Netherlands. In: Proceedings of Symposium on River, Coastal and Estuarine Morphodynamics, Genova, Italy, 2, pp. 705–714.

Koch, M., Niemeyer, H.D., 1978. Sturmtiden-Strommessungen im Bereich des Norderneyer Seegats. Forschungsstelle Norderney, Jahresbericht Nr 29, 91–108.

Kraus, N.C., 2000. Reservoir model of ebb-tidal shoal evolution and sand bypassing. J. Waterw. Port, Coast. Ocean Eng. 126 (6), 305–313.

Krögel, F., 1995. Sedimentverteilung und Morphodynamik des Otzumer Ebbdeltas (südliche Nordsee). Senckenberg. Maritima 25 (4/6), 127–135.

Oertel, G.F., 1975. Ebb-tidal deltas of Georgia Estuaries. In: Cronin, L.E. (Ed.), Estuarine Research, vol. 2. Academic Press, New York, pp. 267–276.

Pearson, S.G., van Prooijen, B.C., Poleykett, J., Wright, M., Black, K., Wang, Z.B., 2021. Tracking fluorescent and ferrimagnetic sediment tracers on an energetic ebb-tidal delta to monitor grain size-selective dispersal. Ocean Coast Manag. 212, 105835. https://doi.org/10.1016/j.ocecoaman.2021.105835 (this issue).

Pearson, S.G., Verney, R., van Prooijen, B.C., Tran, D., Hendriks, E.C., Jacquet, M., Wang, Z.B., 2021a. Characterizing the composition of sand and mud suspensions in coastal and estuarine environments using combined optical and acoustic measurements. J. Geophys. Res.: Oceans 126, e2021JC017354. https://doi.org/10.1029/2021JC017354.

Ridderinkhof, W., Hoekstra, P., van der Vegt, M., de Swart, H.E., 2016. Cyclic behaviour of sandy shoals on the ebb-tidal deltas of the Wadden Sea. Continent. Shelf Res. 115, 14–26. https://doi.org/10.1016/j.csr.2015.12.014.

Sha, L.P., 1989. Variation in ebb-tidal delta morphologies along the west and East Frisian Islands, The Netherlands and Germany. Mar. Geol. 89, 11–28.

Spanhoff, R., Biegel, E.J., van de Graaff, J., Hoekstra, P., 1997. Shoreface nourishment at Terschelling, The Netherlands: feeder berm or breaker berm? In: Thornton, E.B. (Ed.), Proceedings 3rd International Conference on Coastal Dynamics '97. American Society of Civil Engineers, New York, pp. 863–872.

Stive, M.J.F., de Schipper, M.A., Luijendijk, A.P., Aarninkhof, S.G.J., van Gelder-Maas, C., van Thiel de Vries, J.S.M., de Vries, S., Henriquez, M., Marx, S., Ranasinghe, R., 2013. A new alternative to saving our beaches from sea-level rise: the Sand Engine. J. Coast Res. 29 (5), 1001–1008. https://doi.org/10.2112/JCOASTRES-D-13-00070.1.

Tanczos, I.C., Aarninkhof, S.G.J., Van der Weck, A.W., 2000. Ruimte voor de Zandrivier (in Dutch). WL|Delft Hydraulics, Delft. Report Z3200.

Van der Werf, J., Álvarez Antolínez, J.A., Brakenhoff, L., Gawehn, M., den Heijer, K., de Looff, H., van Maarsseveen, M., Meijer - Holzhauer, H., Mol, J., Pearson, S., van Prooijen, B., Santinelli, G., Schipper, C., Tissier, M., Tonnon, P.K., de Vet, L., Vermaas, T., Wilmink, R., de Wit, F., 2019. Data Report Kustgenese 2.0 Measurements. Report 1220339-015. Deltares, Delft, p. 116.

Van Prooijen, B.C., Tissier, M.F.S., de Wit, F.P., Pearson, S.G., Holzhauer, H., Gawehn, M., Antolínez, J.A.A., de Vet, P.L.M., Reniers, A.J.H.M., Wang, Z.B., den Heijer, C., Wilmink, R.J.A., 2020. Measurements of hydrodynamics, sediment, morphology and benthos on Ameland ebb-tidal delta and lower shoreface. Earth Syst. Sci. Data 12 (4), 2775–2786. https://doi.org/10.5194/essd-12-2775-2020.

Van Sijp, D., 1989. Correcties op Gemeten Eb- en Vloedvolume bij Omrekening naar Gemiddeld Getij in het Friesche Zeegat. Report ANW 89-02 (in Dutch). Rijkswaterstaat, Directie Friesland, Leeuwarden.

van Weerdenburg, R., Pearson, S., van Prooijen, B., Laan, S., Elias, E., Tonnon, P.K., Wang, Z.B., 2021. Field measurements and numerical modelling of wind-driven exchange flows in a tidal inlet system in the Dutch Wadden Sea. Ocean Coast Manag. 215, 105941. https://doi.org/10.1016/j.ocecoaman.2021.105941 (this issue).

Walton, T.L., Adams, W.D., 1976. Capacity of inlet outer bars to store sand. In: Proceedings 15th Coastal Engineering Conference, Honolulu, Hawaii. American Society of Civil Engineers, New York, pp. 19–37.

Wang, Z.B., Hoekstra, P., Burchard, H., Ridderinkhof, H., De Swart, H.E., Stive, M.J.F., 2012. Morphodynamics of the Wadden Sea and its barrier island system. Ocean Coast Manag. 68, 39–57.

Zijderveld, A., Peters, H., 2006. Measurement program Dutch Wadden Sea. In: Proceedings 30th International Conference on Coastal Engineering. American Society of Civil Engineers, New York, pp. 404–410. San Diego, USA.